

## HIGH-VELOCITY IMPACTS ON AEROSPACE THIN COMPOSITE LAMINATES

Consuelo Terra<sup>\*</sup>, Michele Pasquali<sup>†1</sup>, Paolo Gaudenzi<sup>†2</sup>

<sup>\*</sup>PhD Candidate at the Department of Mechanical and Aerospace Engineering  
University of Rome, La Sapienza (Italy)  
terra.consuelo@gmail.com

<sup>†1</sup>Research associate at the Department of Mechanical and Aerospace Engineering  
University of Rome, La Sapienza (Italy)  
michele.pasquali@uniroma1.it

<sup>†2</sup>Full professor at the Department of Mechanical and Aerospace Engineering  
University of Rome, La Sapienza (Italy)  
paolo.gaudenzi@uniroma1.it

**Key words:** Analytical model, High-velocity impact, Ballistic limit, Composite target, Stress wave.

**Summary:** *Even though polymer matrix composites generally possess high specific stiffness and high specific strength, they feature a reduced ability to absorb impact energy. Structures subjected to high velocity impacts (HVI), therefore, are likely to suffer complete perforation, which, in the aerospace field, can lead to the dramatic failure of the overall structural system. The effective use of composite materials in structural aerospace applications is thus critically affected by the capability of ascertaining their performances when subjected to impacts. In this work, an analytical formulation aimed at estimating the ballistic limit of thin composite targets given their mechanical and geometric properties, as well as the projectile shape and initial velocity, is proposed. The described approach, in particular, takes into account two-dimensional woven fabric composites and it is based on wave propagation theory. In the impact event, an energy transfer from the projectile to the target takes place. The kinetic energy of the projectile is either absorbed or dissipated by the composite laminate via various deformation/damage mechanisms. Among them, (i) the tensile deformation of the yarns lying in the area of the impact (primary yarns); (ii) the deformation of yarns constituting the region surrounding the impacted zone (secondary yarns); (iii) the delamination onset and propagation and (iv) the matrix cracking play a critical role. Additionally, while thin and flexible composites show a conical deformation on the back face of the target with kinetic energy associated to the moving cone, thick and rigid composites are mainly affected by shear plugging. Here, in particular, an innovative formulation to describe the effects associated to the shear plugging is developed. Finally, the ballistic limit, the damage size and the impact duration are obtained through enforcement of the energy balance. A validation of the proposed formulation is achieved resorting to an experimental campaign as well as to literature results. The obtained numerical predictions are found to be in good agreement with the experimental data.*

## 1 INTRODUCTION

Resistance to ballistic impacts is a key requirement for an effective use of composite structures in many engineering applications. In particular, when survivability of personnel and equipment against penetration by external objects is required, 2D woven fabrics are known to represent the best option in terms of impact performance [1-3].

A clear understanding of the phenomena which characterize the impact of a projectile on a composite woven fabric laminate is a mandatory step towards the effective mathematical representation of impact events. As a general statement, impacts can be grouped into three classes: low-velocity, high-velocity and hyper-velocity impacts [10]. Such classification is driven by the different energy transfer phenomena which take place between the projectile and the target as the initial velocity of the projectile varies, with energy dissipation and damage propagation mechanisms undergoing drastic changes. Low-velocity impacts are characterized by a contact period with the impactor which is longer than the time period of the lowest mode of vibration of the target [15]. In low-velocity impact regime, boundary conditions largely influence the response of the system to the impact. Stress waves generated outward from the impact point, in fact, have enough time to reach the boundaries of the structure, resulting into a dynamic response which involves the complete target. In high-velocity impact conditions, on the contrary, the response of the structure is governed by the behavior of the material in the neighborhood of the impacted zone, with the impact response of the target being not influenced by its boundary conditions. In this case, the contact period of the projectile is much smaller than the time period of the lowest mode of vibration of the structure, so that no information associated to the impact event can reach the boundaries of the target [15]. In hyper-velocity impacts, finally, the projectile velocity assumes values such that the target locally behaves like a fluid (in as so-called *hydrodynamic analogy*), with induces stresses which exceed the material strength by several orders of magnitude [16].

Ballistic impact is generally a low-mass high-velocity impact caused by a propelling source. Among different possible definitions, ballistic limit of a target can be introduced as the maximum velocity of a projectile at which the complete perforation takes place with zero exit velocity [15].

The objective of the current work is to present an analytical formulation for the ballistic impact analysis relying on the geometric and the elastodynamic characteristics of the target, with particular reference to the properties defining the damage mechanisms onset and propagation. In the same way, the projectile mass, velocity, shape and size are taken into account. The studies have been presented for typical woven fabric carbon/epoxy composites impacted with flat-end cylindrical projectiles. In particular, the case of thin fiber reinforced composite targets possessing high specific strength is also considered. Despite their thin nature, for such specimens (which are representative of a large body of engineering applications, above all in the lightweight armor systems field [1, 2]), the effects associated to impact-induced shear stresses are nontrivial, making the description of shear wave propagation in the target through-the-thickness direction a necessary step. Using the proposed formulation, the energy absorbed by different damage and energy absorbing mechanisms, the ballistic limit, the contact duration and the damage size are estimated. Numerical predictions are finally discussed via a comparison with literature and experimental results.

## 2 ANALYTICAL FORMULATION

A ballistic impact is usually a low-mass, high-velocity impact of a projectile onto a target. Given the high velocities involved in the event, the effects on the target stay confined to the region of impact, with an energy transfer taking place from the projectile to the target. Depending on the mechanical and kinematic parameters characterizing the projectile-target pair, a ballistic impact can result into three different scenarios: (i) the projectile completely perforates the target and exits with non-null residual velocity; (ii) the projectile partially penetrates the target, either remaining stuck within it or rebounding; (iii) the projectile completely perforates the target with zero exit velocity. In case (i) the projectile initial (kinetic) energy is larger than the energy the target can either absorb or dissipate: the opposite occurs in (ii). In the last scenario, instead, all the kinetic energy possessed by the impactor is transferred to the target, matching the largest amount of energy the target can receive and absorb/dissipate. In such condition, the initial velocity of the projectile of a given mass is termed as *ballistic limit*. The physical principles along with the modeling assumptions considered to proceed with the analytical description of these phenomena are described in this section.

### 2.1 Basic Assumptions

The energy transfer characterizing cases (i)-(iii) is defined by different energy absorbing/dissipating mechanisms occurring in the target. Possible energy absorbing mechanisms are: cone formation, tension and fracture of primary yarns (see Fig.1), deformation of secondary yarns, delamination onset and propagation, matrix cracking, shear plugging and friction between the projectile and the target [9, 10]. Given the inner complexity of such mechanisms, some physical assumptions have to be made to enable a simplified and yet accurate modelling. The present mathematical formulation is based on the following assumptions:

1. The projectile is assumed to be undeformable, cylindrical, with flat end;
2. During the impact event, the projectile is always in contact with the target. This implies that it is stitched to a constant number of primary yarns, so that the zone of primary yarns is constant and limited by the diameter of the projectile. This assumption is well adapted to cylindrical projectiles with flat end;
3. The projectile-target motion is uniform in each time interval of the contact period;
4. The interactions among layers, among yarns, and between yarns and the projectile are trivial and are therefore neglected, so that each layer and yarn is considered to act independently;
5. The projectile trajectory is orthogonal to the target;
6. Longitudinal and transverse waves originate from the edge of the projectile.

Additional assumptions are associated to the specific nature of the target to be investigated and directly affect the balance of the energy transferred from the impactor to the laminate.

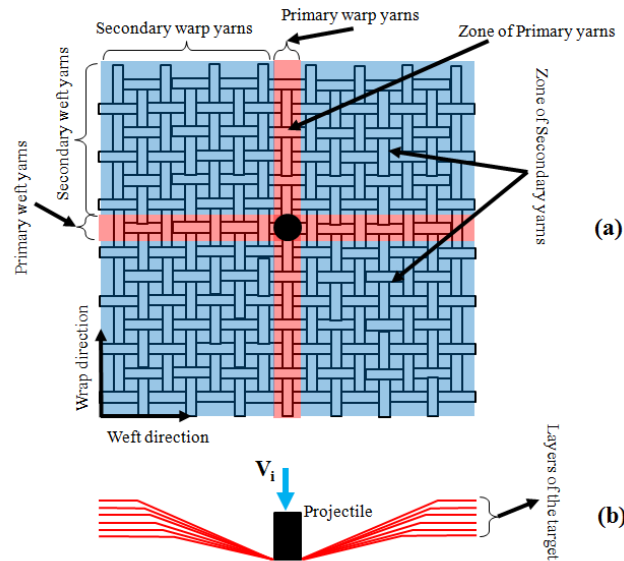


Figure 1: Front (a) and side (b) view of a thin woven target.

## 2.2 Energy Balance

For different materials like carbon, glass or Kevlar, different energy-absorbing/damage mechanisms can prevail. Moreover, the reinforcement architecture can influence the energy absorbing mechanisms. One additional parameter governing the behavior of the target is its stiffness. For thin and/or low-Young's modulus specimens, yarns deformation and fracture generally represent the dominant energy absorbing mechanism [17]. No through-the thickness propagation of elastic waves is usually taken into account in this case. Thick targets, instead, are characterized by the onset of compression waves propagating in the target thickness direction, with the formation of a plug beneath the projectile due to shear stresses which move through the target [18]. The elastic waves propagation along the target thickness direction must be considered in such scenario.

The case here addressed is represented by thin glass fiber and carbon fiber laminates, which find use in many engineering applications and exhibit features belonging both to thin/flexible and thick/stiff targets. Due to their reduced thickness, this type of composites can experience large deflections as a consequence of the impact, causing severe deformation of the yarns. On the other hand, however, the brittle nature of the carbon fibers and their high Young's modulus cause the formation of a plug beneath the projectile in the very first instants of the impact event.

Therefore, the energy transfer from the projectile to the target is defined by six energy-absorbing/dissipating mechanisms: (i) cone formation on the back face of the target; (ii) tensile failure of primary yarns; (iii) deformation of secondary yarns; (iv) shear-plugging; (v) delaminations onset and (v) growth; (vi) matrix cracking. During the ballistic impact event, the energy associated to the projectile-target pair must match in every instant of time the kinetic energy possessed by the projectile before the impact. Enforcing the energy conservation, the following holds:

$$E_0^{KP} = E_i^{KP} + E_i^{KC} + E_{(i-1)}^{PY} + E_{(i-1)}^{SY} + E_{(i-1)}^{SP} + E_{(i-1)}^{DL} + E_{(i-1)}^{MC} \quad \text{for } i = 1, \dots, I \quad (1)$$

where  $E_0^{KP}$  is the kinetic energy of the projectile just before it comes in contact with the target;  $E_i^{KP}$  and  $E_i^{KC}$  are the kinetic energies of the projectile and of the conical region of the target interested by transverse waves propagation at the  $i$ -th time interval, respectively;  $E_{(i-1)}^{PY}$  represents the energy dissipated by the fracture of primary yarns and  $E_{(i-1)}^{SY}$  is the impact energy absorbed by deformation of the secondary yarns until the  $i-1$ -th instant of time;  $E_{(i-1)}^{SP}$  is the energy dissipated via shear-plugging;  $E_{(i-1)}^{DL}$  and  $E_{(i-1)}^{MC}$  are the energy absorbing contributions due to delamination and matrix cracking until the same instant  $i-1$ ; finally,  $I$  is the last instant of time of the impact. Given that  $E_{(0,i)}^{KP} = \frac{1}{2}m_p V_{(0,i)}^2$  and  $E_i^{KC} = \frac{1}{2}m_c V_i^2$ , where  $m_p$  and  $m_c$  are the projectile and the cone masses, respectively, and defining

$$E_{(i-1)}^{TOT} = E_{(i-1)}^{PY} + E_{(i-1)}^{SY} + E_{(i-1)}^{SP} + E_{(i-1)}^{DL} + E_{(i-1)}^{MC} \quad (2)$$

the energy balance equation in (1) can be rewritten as

$$\frac{1}{2}m_p V_0^2 = \frac{1}{2}m_p V_i^2 + \frac{1}{2}m_c V_i^2 + E_{(i-1)}^{TOT} \quad (3)$$

From the above equation, the velocity of the projectile (and of the target onto which the projectile is stitched) can be obtained as

$$V_i = \sqrt{\frac{m_p V_0^2 - 2E_{(i-1)}^{TOT}}{m_p + m_c}} \quad (4)$$

so that, given the projectile velocity at the previous iteration, its velocity can be obtained for each instant of time as a result of the energy-absorbing/dissipating mechanism occurring in the target. The projectile deceleration can thus be estimated as

$$\Delta\alpha_i = \frac{V_{(i-1)} - V_i}{\Delta t} \quad (5)$$

where  $\Delta t$  is the time step of the algorithm. The contact force  $F_i$  resisting the projectile motion at the  $i$ -th iteration is given by

$$F_i = m_p \Delta\alpha_i \quad (6)$$

while the displacement of the conical region of the target due to the impact at each time interval finally reads

$$\Delta h_i = V_{(i-1)} \Delta t - \frac{1}{2} \Delta\alpha_i \Delta t^2 \quad (7)$$

### 3 DEFORMATION OF THE TARGET

In this section, the formation of a cone in the target back surface as well as the deformation and fracture of the laminate yarns under the effects of the impact with the

projectile are described. In particular, the energy associated to the moving cone, the tensile failure of primary yarns and the deformation of secondary yarns are estimated.

### 3.1 Cone Formation

The information of a projectile impacting the target propagates in the laminate under the form of strain waves. Given the above hypotheses, in-plane-propagating waves are assumed to originate from the projectile circumference to travel in the radial direction. Such waves are characterized by a polarization direction which is either parallel or normal to the direction of propagation for the case of longitudinal and transverse waves, respectively. The generation and propagation of the latter, in particular, is associated to the formation of a conical region around the impact point which translates with the projectile [13, 19]. Given the dependence on the orientation of the elastic properties and of the critical strain energy release rates, a lemniscate shape is expected for the cone: for the sake of simplicity, however, the cone is here considered to be of circular cross-section. To estimate the kinetic energy related to the moving cone, the area traveled by transverse wave must be calculated. For these waves, the propagation velocity through an infinitesimal region of the target characterized by the strain and stress values  $\bar{\varepsilon}$  and  $\bar{\sigma}$ , respectively, reads [8]:

$$c_t = \sqrt{\frac{(1 + \bar{\varepsilon})\bar{\sigma}}{\rho} - \int_0^{\bar{\varepsilon}} \frac{1}{\rho} \left( \frac{d\sigma}{d\varepsilon} \right) d\varepsilon} \quad (8)$$

where  $\rho$  is the target density. The distance traveled by transverse waves is

$$r_{ti} = \sum_{k=1}^{k=i} c_{tk} \Delta t \quad (9)$$

so that the mass of the conical region of the target at the  $i$ -time instant can be estimated as  $m_{ci} = \rho h \pi r_{ti}^2$ , where  $h$  is the overall thickness of the target. The kinetic energy associated to the moving cone finally reads

$$E_i^{KC} = \frac{1}{2} m_c V_i^2 \quad (10)$$

### 3.2 Primary Yarns

When a yarn is impacted by the projectile, longitudinal strain waves propagate outwards along the filament [7, 8]. The innermost and outermost longitudinal waves propagating in the target when it is undeformed or it has undergone plastic deformation, respectively, have velocities

$$c_l^{e,y} = \sqrt{\frac{1}{\rho} \left( \frac{d\sigma}{d\varepsilon} \right)_{\varepsilon=0, \varepsilon_y}} \quad (11)$$

and are termed *elastic* and *plastic* wave. The distance traveled by such waves at the  $i$ -th instant of time is  $r_{li}^e = ic_l^e \Delta t$  and  $r_{li}^y = ic_l^y \Delta t$ . While propagating, longitudinal waves suffer

an attenuation which is mainly due to the phenomenon of wave reflection and transmission as the wave encounters material boundaries [7]. The studies carried out on wave attenuation of longitudinal waves during ballistic impact on typical woven fabric composites based on wave reflection/transmission at the interfaces showed that the distribution of the normalized stress  $\sigma^*$  along the yarns directly below the projectile, known as primary yarns, is of the type [9]

$$\sigma^*(x) = b \bar{a}^{\frac{x}{a}} \quad (12)$$

where  $b$  is referred to as *transmission factor* and it assumes positive values smaller than 1,  $x$  is the distance from the impact point and  $a$  is the yarn size. The transmission factor  $b$  is a material property and depends on the geometry of the fabric as well as on the mechanical and physical properties of the reinforcing material and the matrix. As a result of stress wave attenuation from the point of impact up to the point where the longitudinal stress wave has reached, there would be strain variation also, namely [9]

$$\varepsilon(x) = \varepsilon_0 \bar{a}^{\frac{x}{a}} \quad (13)$$

where  $\varepsilon_0$  is the strain at point of impact. The elongation is representative of the material flow along the thickness direction caused by the impact (see Fig. 2). From the definition of the Cauchy strain,  $\varepsilon = (dl - dL)/dL$ , with  $L$  and  $l$  representing the reference and actual length of an infinitesimal material fiber of the domain. Integrating this expression with (13), the strain at  $x = 0$  at the  $i$ -th time instant reads

$$\varepsilon_{0i} = \frac{L_i - l_i}{\frac{l_i}{a} (b \bar{a}^{\frac{l_i}{a}} - 1)} \ln(b) \quad (14)$$

with  $L_i$  and  $l_i$  representing the final and initial length of the primary yarn. If the transverse motion of the target under the action of the projectile is therefore taken into account, the distance traveled by the plastic wave at the  $i$ -th instant of time can be considered as representative of the length of the (transversely) undeformed primary yarn, namely,  $L_i = r_{pi}$ . On the other hand, the actual length of the primary yarn can be obtained observing Fig.3 as  $l_i = \frac{d}{2} + \sqrt{\left(r_{ti} - \frac{d}{2}\right)^2 + h_i^2} + (r_{pi} - r_{ti})$ , where  $h_i$  is the distance traveled by the projectile at the  $i$ -th instant of time. The expression of  $\varepsilon_{0i}$  finally becomes

$$\varepsilon_{0i} = \frac{\frac{d}{2} + \sqrt{\left(r_{ti} - \frac{d}{2}\right)^2 + h_i^2} - r_{ti}}{\frac{l_i}{a} (b \bar{a}^{\frac{l_i}{a}} - 1)} \ln(b) \quad (15)$$

The tension in primary yarns is directly affected by the portion of the yarns which is in contact with the projectile. According to this, the primary yarn passing below the center of the projectile experiences the largest strain, namely,  $\varepsilon_{0i}$ , as it is in contact with the whole diameter of the impactor (which is assumed to have a flat end by hypothesis). Approaching point A in Fig.4, such strain therefore decreases quadratically with  $y$  ( $y \in [0, \frac{d}{2}]$ ) to a value  $\varepsilon_{Ai}$ .

Additional hypotheses regard the variation of the strain along the thickness of the target. Due to the compression of the layers induced by the impact, in fact, they undergo different elongations. To model this effect, the distance traveled by the projectile after the impact can be expressed as the sum of two contributions: the displacement of the projectile at the target surface  $h_i$ , and an additional term dependent on the coordinate  $\zeta$  along the specimen thickness due to compression. Given the assumption of thin target, a linear dependence on  $\zeta$  of the second term is considered.

As the value of dynamic tensile failure strain  $\varepsilon_r$  is reached in a particular yarn, failure occurs. As a result, if the kinetic energy of the projectile is large enough, a sequential failure of yarns starting with the yarns in the top layer and proceeding towards the bottom layer can be obtained. The elastic energy dissipated by failure of a primary yarn therefore reads

$$e_i^{PY} = 2\pi a^2 \int_0^{r_{pi}} \int_0^{\varepsilon=\varepsilon_r} \sigma(x) d\varepsilon dx \quad (16)$$

so that the total energy dissipated by primary yarns failure is

$$E_i^{PY} = N_i^r e_i^{PY} \quad (17)$$

with  $N_i^r$  representing the number of broken primary yarns at the  $i$ -th time instant.

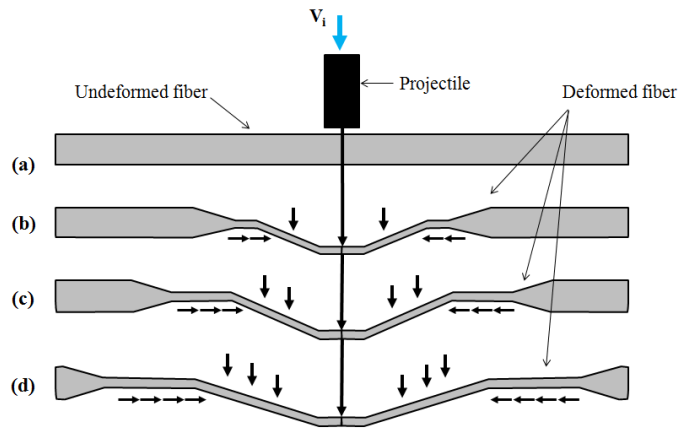


Figure 2: Schematization of a yarn before (a) and after (b, c, d) the impact.

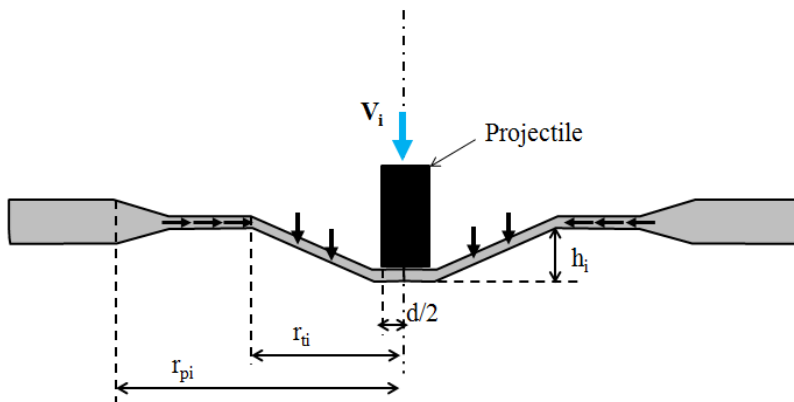


Figure 3: Deformed configuration of a yarn after a high-velocity impact.

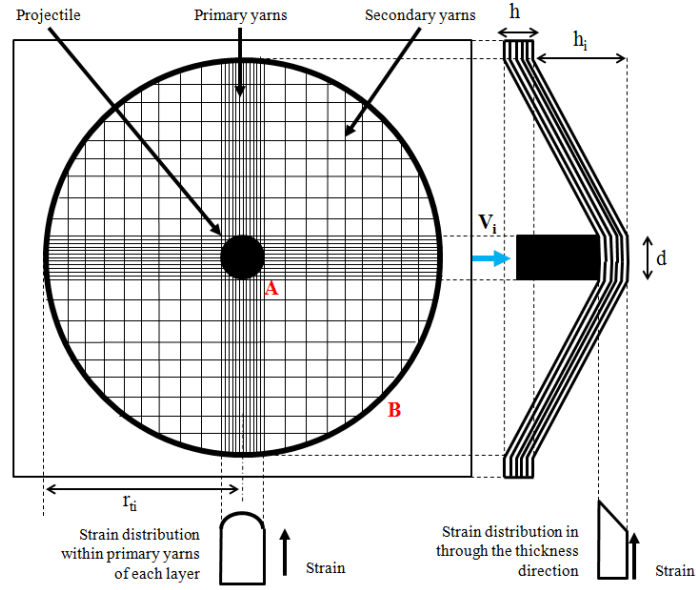


Figure 4: Front and side view of a target subject to impact and representation of the strain distribution within primary yarns of each layer and in through the thickness direction.

### 3.3 Secondary Yarns

Secondary yarns constitute the region of the target traveled by transverse waves with the exception of the area of impact, as shown in Fig.1. Differently from primary yarns, secondary yarns do not break under the effects of the tensile stresses induced by the impact. The kinetic energy of the projectile transferred to the target is partially absorbed by secondary yarns via their elongation as elastic energy. In order to proceed with an estimation of the impact energy absorbed by secondary yarns, a variation of the strain  $\varepsilon$  in the radial direction must be assumed. Imposing the deformations continuity, a value of the strain equal to that experienced by the outermost primary yarns in point A in Fig. 3 is considered for secondary yarns. A null value of the strain is then assumed at the wavefront of the transverse wave in point B. It is hypothesized a linear variation of the strains between points A and B [9].

The elastic energy absorbed by the secondary yarns therefore reads

$$E_i^{SY} = \int_{d/\sqrt{2}}^{r_{ti}} \int_0^{\varepsilon(r)_i} \sigma(r) [2\pi r - 8 \sin^{-1}(d/2r)] h dr d\varepsilon \quad (18)$$

where  $[2\pi r - 8 \sin^{-1}(d/2r)] h dr$  is the infinitesimal volume of the annular region comprised between the circumferences of radius  $r$  and  $r + dr$  and having depth  $h$ .

## 4 DAMAGE MECHANISMS

When the ballistic limit is reached for a projectile-target pair, the energy transferred from the projectile to the target during the impact is partially absorbed by the target (via the deformation mechanisms above described), while the rest is dissipated through the onset and

growth of damages in the impacted specimen. The damage scenarios, in particular, are eventually characterized by the presence of delamination, matrix cracking and shear-plugging, as described in the following.

#### 4.1 Matrix Cracking

The variation of the strains in the target along the radial direction considered in the previous section is consistent with the idea, confirmed by experimental data, that the values of deformation for the target decrease with the distance from the point of the impact [20]. Therefore, being driven by the strain induced in the specimen, the presence of cracks in the matrix is confined to a limited region of the target around the point of impact, namely, where the strain exceed a threshold value  $\varepsilon^{MC}$  which is characteristic of the laminate. Defining  $r_i^{MC}$  as the radius of the target area where the strain is larger than the value of matrix cracking onset  $\varepsilon^{MC}$ , the energy dissipated by matrix cracking during the  $i$ -th time interval is

$$\Delta E_i^{MC} = \chi^{MC} e^{MC} V_m S_{an} \pi \left[ (r_i^{MC})^2 - (r_{i-1}^{MC})^2 \right] h \quad (19)$$

where  $\chi^{MC}$  is the percent of cracked matrix with respect to the whole volume,  $e^{MC}$  is the energy dissipated by matrix cracking per unit volume,  $V_m$  is the matrix volume fraction and  $S_{an}$  is a factor taking into account the non-perfect circularity of the cracked area due to the anisotropy of the target. The entire energy dissipated by matrix cracking until the  $i$ -th time instant reads

$$E_i^{MC} = \sum_{n=1}^{n=i} \Delta E_n^{MC} \quad (20)$$

#### 4.2 Delamination

The portion of the target where the strain values exceed the delamination initiation threshold strain  $\varepsilon^{DL}$  undergoes damage in the form of delamination. Due to matrix cracking, the interlaminar strength of the composite decreases so to produce the delaminations onset and propagation for larger deformations. This delamination is of mode II type. As for the case of matrix cracking, delamination does not necessarily manifest at all the laminate interfaces. Defining  $r_i^{DL}$  as the radius of the target area where the strain is larger than the value of delamination onset  $\varepsilon^{DL}$ , the energy dissipated by delamination during the  $i$ -th time interval is

$$\Delta E_i^{DL} = \chi^{DL} G_{II} S_{an} \pi \left[ (r_i^{DL})^2 - (r_{i-1}^{DL})^2 \right] h \quad (21)$$

where  $\chi^{DL}$  is the percent of delaminated area with respect to the whole surface,  $G_{II}$  is the strain energy release rate for delamination in mode II. The entire energy dissipated by matrix cracking until the  $i$ -th time instant reads

$$E_i^{DL} = \sum_{n=1}^{n=i} \Delta E_n^{DL} \quad (22)$$

In most of the analytic formulations of high-velocity impacts on composite laminated target, it is usually assumed that, for the sake of simplicity,  $\varepsilon^{MC} = \varepsilon^{DL}$ , implying that  $r_i^{MC} = r_i^{DL} = r_d$  [9, 10, 18].

### 4.3 Shear Plugging

The contact force generated during the impact event causes the onset of shear waves which propagate from the circumference of the area directly impacted by the projectile. The consequent stresses can shear and push forward the material situated beneath the projectile, so as to generate a hole into which a plug moves towards the back face of the target. The shear induced by the contact force  $F_i$  on the target is usually estimated as the ratio between such force and the sheared surface, namely [21]

$$\tau_i = \frac{F_i}{\pi d h} \quad (23)$$

so that shear plugging occurs in the  $n_i^{SP}$  layers when a limit value  $\tau^{SP}$  is exceeded at the  $i$ -th instant of time.

Different limitations can be found in the above formulation of the shear plugging. The assumption of constant shear in the whole target thickness implied by Eq. (23), in fact, is hardly compatible with the hypothesis of an increasing number of sheared layers  $n_i^{SP}$ . Moreover, this formulation does not take into account the effects of primary yarns failure induced by tension, which directly affects the number of layer actively resisting to shear plugging.

Given the shear modulus of the target  $G_i$ , the velocity of the shear wave propagating in the target thickness direction is  $c_i^\tau = \sqrt{G_i/\rho}$  so that the shear stress induced by the impact just beneath the projectile at the  $i$ -th instant of time reads

$$\tau_i = \frac{F_i}{\pi d c_i^\tau \Delta t} \quad (24)$$

where  $\Delta t$  is the time step. The value of  $G_i$  can be estimated from the stress-strain curve as  $G_{i-1} = \left. \frac{d\tau}{d\gamma} \right|_{\gamma_{i-1}}$  with  $\gamma_0 = 0$  for  $i = 1$ . The expression in Eq. (24) can be used to check the value of the shear in the region of the shear plugging onset. If such value overcomes  $\tau^{SP}$ , then the shear-plugging occurs and the energy dissipated during a time interval is

$$\Delta \bar{E}^{SP} = \tau^{SP} \pi d (c^{\tau SP} \Delta t)^2 \quad (25)$$

so that the energy dissipated until the  $i$ -th time instant is

$$\bar{E}_i^{SP} = \sum_{n=1}^{n=i} \Delta \bar{E}_i^{SP}, \quad \text{with} \begin{cases} \Delta \bar{E}_i^{SP} = 0, & \text{for } \tau_i < \tau^{SP} \\ \Delta \bar{E}_i^{SP} \neq 0, & \text{for } \tau_i \geq \tau^{SP} \end{cases} \quad (26)$$

Following this approach, the energy required for a layer to fail by shear plugging is  $E_r^{SP} = \tau^{SP} \pi h_i^2$ . The number of broken layers at the  $i$ -th time instant is depends on the ratio

between the energy associated with the failure shear wave and the energy required to break a layer by shear plugging, therefore

$$\eta_i^{SP} = \text{Int} \left[ \bar{E}_i^{SP} / E_r^{SP} \right] \quad (27)$$

where  $\text{Int}[\cdot]$  denotes that only the integer part of the fraction is considered. The following condition must hold

$$\eta_i = \eta_i^{SP} + \eta_i^{PY} \leq N \quad (28)$$

where  $\eta_i$  is the total number of broken layers and  $N$  is the number of layers of the target. Equation (28) allows to reformulate the expression in Eq. (24) taking into account the number of layers which at the  $i$ -th time instant already failed due to tension or shear plugging, as

$$\tau_i = \frac{F_i}{\pi d c_i^\tau \Delta t + \eta_i h_i} \quad (29)$$

The energy dissipated in the failure at the  $i$ -th time instant of  $\eta_i^{SP}$  layers due to shear plugging finally reads

$$E_i^{SP} = \eta_i^{SP} E_r^{SP} \quad (30)$$

The condition in (29) is no more fulfilled as the contact force  $F_i$  decreases in the final part of the impact. This means that no additional shear waves with a critical value of the stress  $\tau^{SP}$  are generated. The only contribution to the energy dissipated by shear plugging derives from the shear waves which are still propagating in the target thickness carrying the information  $\tau = \tau^{SP}$ . When such waves reach the back surface of the target, shear plugging stops.

## 5 NUMERICAL IMPLEMENTATION

The formulation of the energy-absorbing/dissipating mechanisms occurring in the target during the impact event which has been proposed in the previous sections is here numerically implemented.

The aim of the proposed formulation is to estimate the ballistic limit and the consequent extent of the damaged area for a given projectile-target pair, the target being a thin composite laminate with high-modulus fibers as carbon fibers. At the generic  $i$ -th time instant, the projectile velocity is used to estimate the kinetic energy of the projectile and of the moving cone. In the same way the contact force and the projectile displacement are obtained via Eqs. (6) and (7), respectively. The value of the deformation  $\varepsilon_0$  at the previous iteration is used to obtain the values of  $r_{ti}$  and  $r_{pi}$  via the estimation of the plastic and transverse wave speeds, as shown in (8) and (11), respectively.

The overall value of the energy absorbed/dissipated by the target at the  $i$ -th instant of time  $E_i^{TOT}$  is obtained summing all the contributions associated to the different deformation/damage mechanisms taking place in the target. The value of the projectile velocity  $V_{1+1}$  at the successive time instant is thus estimated via Eq. (4). The whole process is

repeated until either all the layers of the composite target break or the projectile velocity reaches zero. If the first scenario occurs with the projectile having a non-null exit velocity, the value of the initial velocity of the impactor  $V_0^{(1)}$  is decreased so that the second-try initial velocity  $V_0^{(2)} < V_0^{(1)}$  is considered at the next iteration. In the case the target is not completely perforated, which represents the second possibility, the initial velocity  $V_0^{(1)}$  is increased. The algorithm proceeds until a convergence criterion is met.

## 6 RESULTS AND DISCUSSION

The effectiveness of the proposed formulation is tested on different case studies so as to obtain a comparison with alternative literature approaches. An experimental campaign is therefore carried out to validate the numerical predictions. The obtained results are discussed in the following.

### 6.1 Comparison with literature results

Analyses are carried out on a twill-weave T300 carbon/epoxy composite target, with a cylindrical projectile impacting the laminate: mechanical and geometric specs are reported in Table 1.

<b>Projectile</b>	Shape	-	Cylindrical
	Mass [g]	$m_p$	1.8
	Diameter [mm]	$d$	5
<b>Target</b>	Material	-	T300 Carbon/Epoxy
	Matrix volume fraction [%]	$V_m$	50
	Density [ $\text{kg/m}^3$ ]	$\rho$	1400
	Thickness [mm]	$h$	2
	Number of layers	$N$	5
	Fracture strain [%]	$\varepsilon_r$	0.8
	Fracture stress [MPa]	$\sigma_r$	1187
	Young Modulus [GPa]	$E_{\varepsilon=0}$	148
	Fracture shear strain [%]	$\gamma^{SP}$	3.31
	Fracture shear stress [MPa]	$\tau^{SP}$	90
	Shear modulus [GPa]	$G_{\varepsilon=0}$	5.4
	Anisotropy factor	$S_{an}$	0.9
	Transmission factor	$b$	0.950
	Damage initiation threshold [%]	$\varepsilon_d$	0.32
	Strain energy release rate [ $\text{J/m}^2$ ]	$G_{II}$	800
Matrix cracking release rate [ $\text{MJ/m}^3$ ]	$e^{MC}$	0.9	
Yarn width [mm]	$a$	1.70	
<b>Model</b>	Time-step [ $\mu\text{s}$ ]	$\Delta t$	1

Table 1: Input data of the simulations for twill-weave T300 carbon/epoxy targets.

A ballistic limit of  $105 \div 106$  m/s is found, with a damaged area of radius  $r_d = 14.2 \div 13.5$  mm. For  $V_0 = 105$  m/s, most of the projectile energy is first transformed into kinetic energy of the moving cone and then absorbed as deformation energy of secondary yarns (79.25% of the overall energy transferred to the target). A major role in the impact event is played by shear plugging, whose contribution to energy dissipation amounts to 9.12%. The 4 steps noticeable (Fig.5) in the time history of the energy dissipated via shear plugging indicate the failure of 4 out of 5 layers of the target. The values of 6.38% and 5.25% are respectively obtained for the delamination and matrix cracking contribution to energy dissipation. No effect due to primary yarns failure is found in this case: the perforation of the target is completely driven by shear plugging.

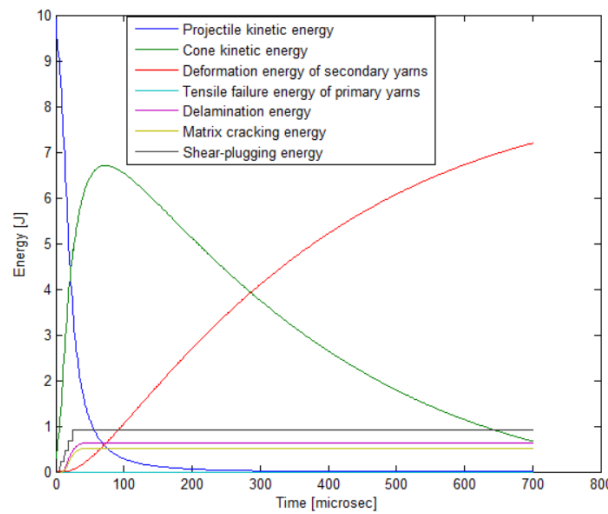


Figure 5: Energy absorbed by twill-weave T300 carbon/epoxy targets through different mechanisms for  $V_i = 105$  m/s.

When the projectile initial velocity is increased to 106 m/s, a residual velocity  $V_R = 51.5$  m/s is obtained. Five steps can now be observed (Fig.6) in the time history of the energy dissipated via shear plugging, indicating complete perforation of the target.

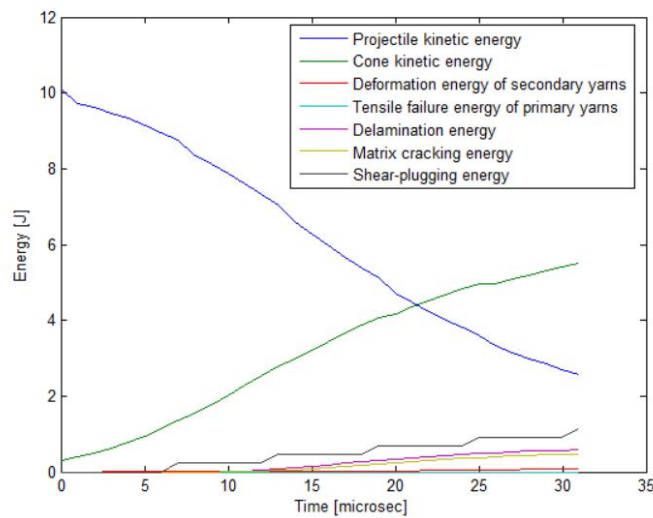


Figure 6: Energy absorbed by twill-weave T300 carbon/epoxy targets through different mechanisms for  $V_i = 106$  m/s.

A comparison with the results obtained in [10] is shown in Table 2 and indicates the accuracy of the proposed approach when nontrivial effects due to the specimen stiffness occur despite its thin nature. While a velocity of 98÷99 m/s is numerically predicted in [10] as ballistic limit, the value of 105m/s is experimentally found, matching the results obtained with the present formulation.

	Current model	Naik et al. [10]	Experiments [10]
Ballistic limit [m/s]	105-106	98-99	105

Table 2: Results for the twill-weave T300 carbon/epoxy targets and comparison with [10].

## 6.2 Experimental tests

The experimental campaign is carried out using plain wave carbon/epoxy multi-layer composite targets whose geometric and mechanical specs are shown in Table 3. The specimens were first manufactured and then tested to determine some of the material parameters required by the semi-analytic formulation: the different phases of the preparation and characterization of the targets are shown in Fig.7.

<b>Projectile</b>	Shape	-	Spherical
	Mass [g]	$m_p$	1.7
	Diameter [mm]	$d$	2.5
<b>Target</b>	Material	-	Carbon/Epoxy
	Matrix volume fraction [%]	$V_m$	58
	Density [ $\text{kg}/\text{m}^3$ ]	$\rho$	1368
	Thickness [mm]	$h$	4
	Number of layers	$N$	25
	Fracture strain [%]	$\varepsilon_r$	1.05
	Fracture stress [MPa]	$\sigma_r$	736
	Young Modulus [GPa]	$E_{\varepsilon=0}$	70.07
	Fracture shear strain [%]	$\gamma^{SP}$	4.30
	Fracture shear stress [MPa]	$\tau^{SP}$	55.5
	Shear modulus [GPa]	$G_{\varepsilon=0}$	2.5
	Anisotropy factor	$S_{an}$	0.9
	Transmission factor	$b$	0.950
	Damage initiation threshold [%]	$\varepsilon_d$	0.42
Strain energy release rate [ $\text{J}/\text{m}^2$ ]	$G_{II}$	800	
Matrix cracking release rate [ $\text{MJ}/\text{m}^3$ ]	$e^{MC}$	0.9	
Yarn width [mm]	$a$	2.50	
<b>Model</b>	Time-step [ $\mu\text{s}$ ]	$\Delta t$	1

Table 3: Input data of the simulations for plain-weave carbon/epoxy targets.

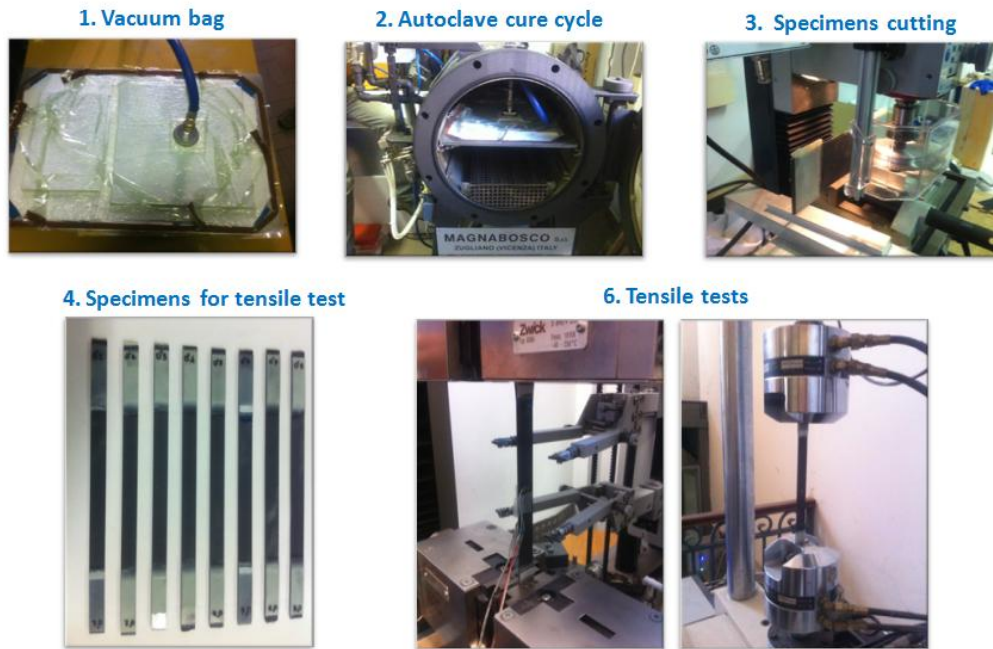


Figure 7: Phases of the preparation and characterization of the targets for the experimental campaign.

A Sabre Ballistics A1G+ gas gun was used to shoot a steel spherical projectile to the targets (see Fig.8). The projectile velocities were acquired using a Photron APX high-velocity camera.



Figure 8: Sabre Ballistics A1G+ Gas gun.

The ballistic limit for the projectile-target pair is numerically found to occur between 181m/s and 182m/s, while a value of 174 m/s is found in the experimental tests [22]. Such difference, however, is mostly ascribable to the different shape of the projectile considered in the tests (a sphere) and in the formulation (a flat-end cylinder). As shown in [11], in fact, decrements up to 7% in the ballistic limit value are observable when a spherical projectile rather than a cylinder is taken into account. The relative importance of the different energy absorbing/dissipating mechanisms is shown in Figs.9 and 10 for  $V_0=181\text{m/s}$  and  $V_0=182\text{m/s}$ , respectively. As observable, the perforation of the target occurs via shear plugging, while no failure of primary yarns is found. The main energy-absorbing mechanism is the deformation of secondary yarns (74.26%), followed by matrix cracking (10.96%), delamination (8.07%) and shear plugging (3.03%). A damaged area of radius  $r_d=19\text{mm}$  is found. The increased importance of the effects associated to matrix cracking and delamination in dissipating the energy of the projectile with respect to the numerical tests results is due to the larger value of the target thickness.

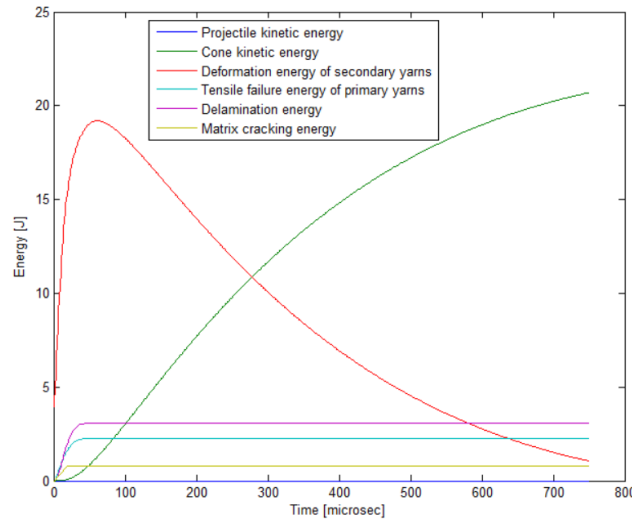


Figure 9: Energy absorbed by the plain-weave carbon/epoxy targets through different mechanisms for  $V_i=181 \text{ m/s}$ .

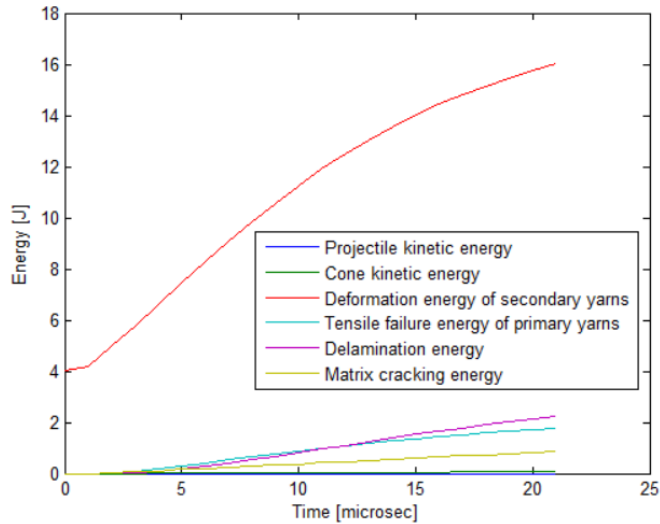


Figure 10: Energy absorbed by the plain-weave carbon/epoxy targets through different mechanisms for  $V_i=182 \text{ m/s}$ .

## 7 CONCLUSION

An analytical formulation to model high-velocity impacts on thin woven fabric composite targets has been presented in this work. The estimation of the ballistic limit for the impactor-target pair has been carried out taking into account the different deformation/damage mechanisms which characterize the target response during the impact event. In particular, the formation of a moving cone in the target, the failure under tension of primary yarns, the elastic deformation of secondary yarns, the onset and propagation of delaminations and matrix cracks and the formation of a plug in the target due to shear stress have been modeled in the proposed formulation as energy-absorbing/dissipating phenomena. The conservation of energy is therefore enforced to drive the transfer of kinetic energy from the projectile to the

target. Resorting to the hypothesis of thin targets, 1D in-plane wave propagation has been considered in the description of all the energy transfer mechanisms, with the exception of shear plugging, for whose formulation through-the-thickness shear waves propagation has been accounted for. This is due to the importance assumed by shear plugging when the case of thin targets characterized by a reinforcement phase possessing a high Young's modulus (e.g. carbon fibers) is considered.

Important deviations from literature formulations were observed for the results obtained for carbon/epoxy composite targets: a velocity of 105-106m/s was obtained as ballistic limit, in comparison with 98-99m/s and 105m/s obtained numerically and experimentally in [9], respectively. Most of the difference with literature results is ascribable to the effects of shear plugging, which was found to cause 9.12% of energy dissipation and, more importantly, to drive the target perforation. No dissipation of energy due to primary yarn failure was noticed for carbon/epoxy targets, as the impact duration was found to be too small in comparison with the time necessary to load the yarns until failure. The proposed formulation has been finally validated through an extensive experimental campaign conducted on carbon/epoxy targets. The velocity of 181-182m/s was estimated as ballistic limit against an experimental value of 174m/s, with the observed difference largely comprised in the deviations ascribable to the projectile shape (cylindrical in the analytical model, spherical in the experiments). Failure of the target was found to occur due to shear plugging. A damaged area of radius  $r_d=19\text{mm}$  was found to occur about the impact point.

## ACKNOWLEDGMENT

The valuable contribution of prof. E. Barbero and Dr. S. Sánchez-Sáez from the Continuum Mechanics Department of Carlos III University of Madrid and of Dr. L. Ferrante from the Chemical, Materials and Environmental Engineering Department of La Sapienza University of Rome in addressing the shooting phase of the experimental campaign is acknowledged.

## REFERENCES

- [1] A. Bhatnagar, *Lightweight ballistic composites military and law-enforcement applications*. In: Bhatnagar A (ed). Woodhead Publishing Limited, Abington Hall, Abington, Cambridge CB1 6AH, England; 2006, pp. 364397.
- [2] JR Vinson, JA. Zukas, *On the ballistic impact of textile body armor*. J Appl Mech 1975;263268.
- [3] M. Grujicic, G. Arakere, *A ballistic material model for cross-plyed unidirectional ultrahigh molecular-weight polyethylene fiber-reinforced armor-grade composites*. Mater Sci Eng 2008;498:231241.
- [4] B. Gu, *Analytical modeling for the ballistic perforation of planar plain-woven fabric target by projectile*. Composites: Part B 2003;34:361371.
- [5] IS. Chocron-Benloulou, J. RodriGuez, V. Sanchez-Galvez, *A simple analytical model to simulate textile fabric ballistic impact behavior*. Text Res J 1997;67:520528.

- [6] M. Mamivand, GH. Liaghat, *A model for ballistic impact on multi-layer fabric targets*. Int J Impact Eng 2010;37:806812.
- [7] B. Parga-Landa, F. Hernandez-Olivares, *An analytical model to predict impact behavior of soft armors*. Int J Impact Eng 1995;16:45566.
- [8] JC. Smith, FL. McCrackin, HF. Scniefer, *Stress-strain relationships in yarns subjected to rapid impact loading*. Part V. Wave propagation in long textile yarns impacted transversely. Text Res J 1958;28:288302.
- [9] NK. Naik, P. Shrirao, BCK. Reddy, *Ballistic impact behaviour of woven fabric composites: formulation*. Int J Impact Eng 2006;32:152152.
- [10] NK. Naik, P. Shrirao, *Composite structures under ballistic impact*. Compos Struct 2004;66:57990.
- [11] HM. Wen, *Penetration and perforation of thick FRP laminates*. Compos Sci Technol 2001;61:116372.
- [12] WL. Cheng, S. Langlie, S. Itoh, *High velocity impact of thick composites*. Int J Impact Eng 2003;29:16784.
- [13] G. Zhu, W. Goldsmith, CK. Dharan, *Penetration of laminated Kevlar by projectiles II. Analytical model*. Int J Solids Struct 1992;29:42136.
- [14] PM. Cunniff, *An analysis of the system effects in woven fabrics under ballistic impact*. Text Res J 1992;62:495509.
- [15] JA. Zukas, T. Nicholas, HF. Swift, LB. Greszczuk, DR. Curran, *Impact Dynamics*. Toronto: John Wiley & Sons, 1982.
- [16] H. Klinkrad, H. Stokes, *Hypervelocity Impact Damage Assessment and Protection Techniques*. In: Klinkrad H, Stokes H (eds) Space Debris. Praxis Publishing Ltd, Chichester, UK; 2006, pp. 199-214.
- [17] C. Ha-Minh, A. Imad, F. Boussu, T. Kanit, *On analytical modelling to predict of the ballistic impact behaviour of textile multi-layer woven fabric*. Compos Struct 2013;99:462-476.
- [18] NK. Naik, AV. Doshi, *Ballistic Impact Behavior of Thick Composites: Analytical Formulation*. AIAA J 2005;43:1525-1536.
- [19] SS. Morye, PJ. Hine, RA. Duckett, DJ. Carr, IM. Ward, *Modelling of the energy absorption by polymer composites upon ballistic impact*. Compos Sci Technol 2000;60:263142.
- [20] G. Zhu, W. Goldsmith, CK. Dharan, *Penetration of laminated Kevlar by projectiles I. Experimental investigation*. Int J Solids Struct 1992;29:399419.

- [21] P. Udata, CVS. Kumar, NS. Nair, NK. Naik, *High velocity impact performance of three-dimensional woven composites*. J. Strain Anal. Eng. Des. 2012;47:419-431.
- [22] J. Tirillò, F. Sarasini, L. Ferrante, T. Valente, L. Lampani, P. Gaudenzi, E. Barbero, E. Sánchez-Sáez, *Effect of basalt fiber hybridization on high velocity impact behavior of carbon/epoxy composites*. Proceedings of the 20th International Conference on Composite Materials (ICCM20), 19-24 July, 2015, Copenhagen, Denmark.